Contents lists available at ScienceDirect

Metabolic Engineering

journal homepage: www.elsevier.com/locate/ymben

Multiplexed site-specific genome engineering for overproducing bioactive secondary metabolites in actinomycetes

Lei Li[a,b]

ZouA and two *oriT*-like recombination sites RsA/RsB mediated tandem amplification of the kanamycin BGC potentially via a rolling circle mechanism in *S. kanamyceticus* (Murakami et al., 2011). Using the ZouA-mediated DNA recombination system, 4–12 tandem copies of the actinorhodin (ACT) BGC and 3–5 copies of the validamycin A (VAL-A) BGC were successfully introduced into the genomes of *Streptomyces coelicolor* M145 and *Streptomyces hygroscopicus* 5008 under antibiotic selection, resulting in 20- and 0.34-fold increases in ACT and VAL-A production, respectively (Murakami et al., 2011; Zhou et al., 2014). However, the tandemly amplified BGCs would be gradually lost in the absence of antibiotic selection (Zhou et al., 2014), suggesting that this method is not suitable for constructing antibiotic hyperproducing strains for large-scale fermentation.

As an attractive alternative, bacteriophage (such as *Φ*C31, *Φ*BT1 and TG1) attachment/integration (Att/Int) systems have been widely exploited for the stable chromosomal integration of target BGCs, thereby enhancing the production of many antibiotics in actinomycetes (Baltz, 2012). In most cases, only one extra copy of target BGCs is introduced by a single Att/Int system, and thus the range of yield improvement is often limited. Recently, two compatible *Φ*C31 and TG1 Att/Int systems were used in a step-by-step manner to duplicate and triplicate the goadsporin BGC, resulting in 1.5- and 2.3-fold increases in goadsporin production of *Streptomyces* sp. TP-A0584, respectively (Haginaka et al., 2014). However, the entire procedure for BGC amplification using different Att/Int systems involves repeated rounds of integrating-plasmid construction and conjugative transfer, and the number of integrated BGCs is also limited by the number of resistance markers available for selection.

Here, we developed a simple and general method for the single-step, multi-copy chromosomal integration of target BGCs via the ‘one integrase-multiple *attB* sites’ concept. We designate this method MSGE (Multiplexed Site-specific Genome Engineering). As a proof-of-concept, multiple artificial *attB* sites (including three artificial *Φ*C31 sites and two artificial *Φ*BT1 *attB* sites) were inserted step by step into the genome2.5111-455.4(B-11.89-2f2213265.4(enhancinr6oy10[d)-237.8(MSGE)]TJ-13.0028-1.3088Td[(l-1.3(PIIp)-56by)-49high-/T10j/Td[(sp.)-355.901 resp

downstream arms of the *cmlR* gene were obtained by PCR using primer pairs *cmlR*-up-fw/rev and *cmlR*-down-fw/rev, respectively, and then ligated together by overlapping PCR using primers *cmlR*-up-fw and *cmlR*-down-rev. The resulting DNA fragment was assembled into Cas9-digested pAH91 with the sgRNA pair *cmlR*-sgRNA-up and *cmlR*-sgRNA-down to generate pAH91Δ*cmlR*. To construct the pAH91*kasO*p*-*cmlR* plasmid, the strong promoter *kasO*p* was introduced when the upstream and downstream arms of the *cmlR* gene were ligated by overlapping PCR.

2.4. Construction of the S. pristinaespiralis and S. coelicolor mutants

The *S. pristinaespiralis* strains SBJ1000::*attB*, SBJ1000::2*attB* and SBJ1000::3*attB* were constructed using the CRISPR/Cas9 genome editing tool (Huang et al., 2015). To generate the SBJ1000::*attB* mutant carrying an in-frame deletion of the first non-target cluster (BGC13, from 4050261 to 4072243, 22 kb) and simultaneous introduction of an artificial *Φ*C31 *attB* site, the upstream and downstream regions of BGC13 were obtained by PCR amplification using primer pairs Del-BGC13-up-fw/rev and Del-BGC13-down-fw/rev, respectively. Using plasmid pCB003 as the template, the sgRNA expression cassette was obtained by PCR amplification with primers BGC13-sgRNA-fw and sgRNA-rev. Then, three DNA fragments were assembled by overlapping PCR with primers BGC13-sgRNA-fw and Del-BGC13-down-rev, and double-digested with *Hin*d III and *Spe* I. The resulting DNA fragment was cloned into pKCCas9 to yield pKCCas9-BGC13. The obtained plasmid was introduced into the parental strain SBJ1000 by conjugal transfer on M-Isp4 medium and the resulting strains were subsequently grown on solid RP medium without apramycin at 37 °C for two rounds to remove plasmid pKCCas9-BGC13. The correct double cross-overs were verified by PCR and sequence analysis with primers ID-BGC13-fw/rev, yielding the SBJ1000::*attB* mutant. Similarly, SBJ1000::2*attB* (containing an in-frame deletion of the second non-target cluster BGC3, from 1106415 to 1130923, 24.5 kb) and SBJ1000::3*attB* (containing an in-frame deletion of the third non-target cluster BGC2, from 686202 to 696578, 10.3 kb) were constructed from SBJ1000::*attB* and SBJ1000::2*attB*, respectively. SBJ1002 and SBJ1003 were obtained by integrating the plasmid BAC-F1F15 into SBJ1000::*attB* and SBJ1000::2*attB*, respectively. The primer pairs ID-native-attB-fw/ID-int-rev, ID-BGC13-attB-fw/ID-int-rev, ID-BGC3-attB-fw/ID-int-rev and ID-BGC2-attB-fw/ID-int-rev were used to track the successful integration of plasmid BAC-F1F15 into the corresponding *Φ*C31 *attB* sites. As a control, the cosmid pAH91 was introduced into SBJ1000::*attB*, SBJ1000::2*attB* and SBJ1000::3*attB* to compare the integration efficiency.

Similarly, SBJ1000::2*attB*::*attBT* (with introduction of *Φ*BT1 *attB* site and simultaneous in-frame deletion of the non-target cluster BGC15, from 5663822 to 5683512, 19.7 kb) and SBJ1000::2*attB*::2*attBT* (with introduction of *Φ*BT1 *attB* site and simultaneous in-frame deletion of the non-target cluster BGC5, from 2056199 to 2066570, 10.4 kb) were constructed from SBJ1000::2*attB* and SBJ1000::2*attB*::*attBT*, respectively. The recombinant plasmid BAC-F1F15(BT-*aphII*) was introduced into SBJ1003 to generate SBJ1004. Next, we constructed SBJ1005 by the step-by-step integration of plasmids BAC-F1F15 and BAC-F1F15(BT-*aphII*) into SBJ1000::2*attB*::*attBT*. The primer pairs ID-oriT-fw/ID-native-BT1-attB-rev and ID-oriT-fw/ID-BGC15-BT1-attB-rev were used to track the successful integration of plasmid BAC-F1F15(BT-*aphII*) into the corresponding *Φ*BT1 *attB* sites.

Finally, we constructed a series of *S. coelicolor* heterologous hosts M1252-M1552 and M1246-M1546 using the CRISPR/Cas9 genome editing method (Huang et al., 2015). To generate the M1252 mutant (containing an artificial *Φ*C31 *attB* site inserted into the location where the CPK BGC was deleted), the upstream and downstream regions of the CPK BGC were obtained by PCR amplification with the primer pairs Del-CPK-up-fw/rev and Del-CPK-down-fw/rev, respectively. Using the plasmid pCB003 as the template, the sgRNA expression cassette was obtained by PCR amplification with primers CPK-sgRNA-fw and sgRNA-rev. Then, three DNA fragments were then assembled by overlapping PCR using primers CPK-sgRNA-fw and Del-CPK-down-rev. The resulting DNA fragment was cloned into pKCCas9 using the one-step cloning kit (Vazyme) to yield pKCCas9-CPK. The obtained plasmid was introduced into the M1152 strain by conjugal transfer on M-Isp4 medium. The correct double cross-overs were verified by PCR using primers ID-CPK-fw/rev, yielding the M1252 mutant. To easily identify the insertion of *Φ*C31 *attB* sites, we knocked out a short DNA region (~500 bp) in the target location where the artificial *attB* site was meant to be inserted. The M1352 mutant (containing two artificial *Φ*C31 *attB* sites and the second *Φ*C31 *attB* site was inserted into the location where the RED BGC was deleted) was constructed from M1252 using the same strategy. The mutants M1452 (containing three artificial *Φ*C31 *attB* sites and the third *Φ*C31 *attB* site was inserted into the location where the CDA BGC was deleted) and M1552 (containing four artificial *Φ*C31 *attB* sites and the fourth *Φ*C31 *attB* site was inserted into the location where the ACT BGC was deleted) were also constructed from M1352 and M1452, respectively. Using M1146 as the starting strain, the M1246-M1546 mutants were obtained using the same procedure applied for M1252-M1552. The cosmid pAH91 (containing the chloramphenicol BGC) was then introduced into M1152-M1552 by conjugal transfer. Similarly, the cosmid pST85 (containing the YM-216391 BGC) was introduced into M1152-M1552 and M1146-M1546. The primer pairs ID-oriT-fw/ID-native-attB-rev, ID-oriT-fw/ID-CPK-attB-rev, ID-oriT-fw/ID-RED-attB-rev, ID-oriT-fw/ID-CDA-attB-rev and ID-oriT-fw/ID-ACT-attB-rev were used to track the successful integration of the cosmid pAH91 or pST85 into the corresponding *Φ*C31 *attB* sites. As a control, plasmid BAC-F1F15 was also introduced into M1152-M1552 to compare the integration efficiency. In each experiment, ten exconjugants were randomly picked to determine the integration efficiency by PCR analysis and the experiments were repeated twice. The primers used are listed in Table S2.

2.5. Pristinamycin II production and microscopic observation of S. pristinaespiralis

Morphological observation, fermentation and analysis of pristinamycin II production were performed as described previously (Li et al., 2015). The data were analyzed by Student's *t*-test, with $*p < 0.05$ indicating significant difference.

2.6. Chloramphenicol production

S. coelicolor fermentation and chloramphenicol production were performed as described previously (Gomez-Escribano and Bibb, 2011). Briefly, M1152-M1452/pAH91 were germinated in 4 mL of 2×YT for 8–10 h at 30 °C and re-suspended in GYM medium (g/L, glucose 4, yeast extract 4, malt extract 10, peptone 1 and NaCl 2, pH 7.2). The cultures were then incubated at 30 °C in 50 mL of GYM medium in a 250-mL shake flask on an orbital shaker (200 rpm). The fermentation samples were harvested at 1, 2, 3, 4 and 5 days, and centrifuged at 12, 000 rpm for 10 min. The supernatants were used to directly analyze chloramphenicol production by HPLC (1260 series, Agilent) using a 4.6×150 mm Zorbax Eclipse XDB-C18 column (Agilent). For HPLC detection, a water: methanol gradient was used as the mobile phase: min 0, 25% methanol; min 2, 25% methanol; min 12, 50% methanol, min 14, 100% methanol; min 20, 100% methanol; min 22, 25% methanol; and min 25, 25% methanol. The flow rate was 1.0 mL/min and chloramphenicol eluted at approximately 11.3 min. The eluate was monitored at 273nm, and the column temperature was 30 °C. The chromatogram of chloramphenicol is presented in Fig. S1a, and chloramphenicol production was calculated from the standard curve (Fig. S1b). The data were analyzed by Student's *t*-test, with $*p < 0.05$

indicating significant difference.

2.7. YM-216391 production

S. coelicolor fermentation and YM-216391 production analysis were performed as described previously (Jian et al., 2012). The fermentation procedure employed for YM-216391 was similar to that used for chloramphenicol. The fermentation samples were harvested at 1, 2, 3, 4 and 5 days, and centrifuged at 12, 000 rpm for 10 min. The mycelia were extracted with the same volume of acetone overnight. The supernatants from fermentation samples and extracted mixtures were used to analyze YM-216391 production by HPLC (1260 series, Agilent) using a 4.6×150 mm Zorbax Eclipse XDB-C18 column (Agilent). For HPLC detection, a water: acetonitrile gradient was used as the mobile phase: min 0, 10% acetonitrile; min 5, 10% acetonitrile; min 25, 95% acetonitrile, min 28, 10% acetonitrile; and min 30, 10% acetonitrile. The flow rate was 1.0 mL/min and YM-216391 eluted at approximately 21.4 min. The eluate was monitored at 287nm, and the column temperature was 30 °C. The chromatogram of YM-216391 is presented in Fig. S2a, and YM-216391 production was calculated according to the standard curve (Fig. S2b). The data were analyzed by Student's *t*-test, with $*p < 0.05$ indicating significant difference.

2.8. RNA preparation and quantitative real-time PCR (qRT-PCR)

RNA preparation and qRT-PCR analysis were performed as described previously (Wang et al., 2013a). The primers used are listed in Table S2. For transcriptional analysis in *S. pristinaespiralis* and *S. coelicolor*, two *hrdB* genes (encoding the corresponding RNA polymerase principal sigma factor), namely *SSDG_06142* (*hrdBspr*) and *sco5820* (*hrdB*), respectively, were used as internal controls. qRT-PCR analysis was performed in triplicate for each transcript and repeated with three independent RNA samples. The relative expression levels of the tested genes were normalized to those of *hrdBspr* or *hrdB*. The relative fold-changes in the expression of each gene were determined using the $2^{-\Delta\Delta Ct}$ method (Livak and Schmittgen, 2001). The data were analyzed by Student's *t*-test, with $*p < 0.05$ indicating significant difference.

3. Results

3.1. Design of the MSGE method

Many actinomycetes typically contain no or only one active *attB* site for each bacteriophage integrase (Baltz, 2012). In theory, the prior introduction of artificial *attB* sites into the actinomycete chromosome could allow the simultaneous integration of multiple copies of target BGCs after a single round of conjugal transfer. Herein, the genomic loci of secondary metabolite BGCs, which do not encode the target products, are named as “non-target BGCs” and chosen for the insertion of artificial *attB* sites, since deletion of the non-target BGCs could possibly facilitate precursor availability and simplify the identification of target products (Gomez-Escribano and Bibb, 2014; Komatsu et al., 2010). Furthermore, genome-reduced actinomycete strains, where non-target BGCs were deleted, could maintain the original scale of the chromosome after amplification of target BGCs, thus avoiding limited chromosome packaging space within the spore (Yanai et al., 2006).

Therefore, we design to knock out the non-target BGCs in two representative antibiotic-producing streptomycetes and simultaneously introduce artificial *attB* sites into the chromosome (Fig. 1), which could be rapidly accomplished using the highly-efficient CRISPR/Cas9 genome editing method (Huang et al., 2015). The experimental setup and procedure are as follows. First, an artificial *attB* site is added between two homology-directed repair templates for deleting a non-target BGC. Then, the CRISPR/Cas9 editing system is employed to rapidly knock out the non-target BGC and simultaneously insert the exogenous *attB* site. Through several rounds of the deletion/insertion process, multiple artificial *attB* sites are discretely introduced into the chromosome of actinomycetes. Finally, after a single round of conjugal transfer, multi-copy target BGCs would be possibly integrated into the native and artificial *attB* sites at the same time (Fig. 1). By this ‘one integrase-multiple *attB* sites’ strategy, we aimed to develop MSGE (Multiplexed Site-specific Genome Engineering) to achieve the single-step, multi-copy chromosomal integration of target BGCs, which may effectively improve production of important secondary metabolites in actinomycetes.

3.2. Validating MSGE for enhanced pristinamycin II (PII) production in S. pristinaespiralis

Pristinamycin produced by *S. pristinaespiralis*, consists of two chemically unrelated molecules, pristinamycin I (PI) and pristinamycin II (PII). PI_A and PII_A are the major forms of PI and PII, respectively. Semi-synthetic derivatives of pristinamycin have been approved to treat a broad range of drug-resistant pathogens (Mast and Wohlleben, 2014). Previously, we employed a combinatorial metabolic engineering strategy involving the duplication of the PII BGC and the systematic engineering of cluster-situated regulatory genes to optimize PII production (Li et al., 2015). The introduction of an extra PII BGC via the ΦC31 Att/Int system led to a significant increase in PII titers by 75% in the recombinant strain Δ*papR5+R4R6* (named SBJ1000), which was generated by deleting the repressor gene *papR5* in combination with overexpression of both activator genes *papR4* and *papR6* (Li et al., 2015). We reasoned that higher-order amplification of the PII BGC may further enhance PII production.

As a proof-of-concept, we aimed to amplify the PII BGC based on the SBJ1000 strain using the MSGE method. By antiSMASH analysis (Weber et al., 2015a), we found that the *S. pristinaespiralis* genome harbours 19 secondary metabolite BGCs with the capacity to produce polyketides (PKs), non-ribosomal peptides (NRPs), terpenes and bacteriocins, etc. (Fig. S31). Considering that pristinamycin biosynthesis is catalysed by a hybrid PKS-NRPS system (Mast et al., 2011), the other three PKS or NRPS BGCs (BGC 2, 3 and 13) were initially chosen as deletion/integration loci (Fig. S3).

First, we deleted the non-target cluster BGC13, and simultaneously inserted an artificial ΦC31 *attB* site into the chromosome via CRISPR/Cas9 genome editing technology. The resulting strain (named SBJ1000::*attB*) was verified by PCR amplification and sequence analysis (Fig. 2a). BGC13 deletion had no obvious effect on PII production (Fig. 2b) and mycelium formation in fermentation medium (data not shown). Next, the plasmid BAC-F1F15 (containing the entire PII BGC) was introduced into SBJ1000::*attB* by intergeneric conjugation. As shown in Fig. S4a, the PII BGC was simultaneously integrated into the native and artificial ΦC31 *attB* sites in SBJ1000::*attB*, showing an insertion efficiency of 100%. This recombinant strain containing two extra copies of the PII BGC was named SBJ1002, and the previously generated SBJ1000/BAC-F1F15 strain (Li et al., 2015) containing an extra copy of the PII BGC was renamed SBJ1001. Fermentation analysis showed that SBJ1002 produced a maximum PII titer of 538 mg/L, which was approximately 17% and 68% higher than SBJ1001 and SBJ1000, respectively (Fig. 2c). These results prompted us to introduce more copies of the PII BGC into the *S. pristinaespiralis* genome for PII titer improvement.

For this purpose, two more artificial *attB* sites were introduced into the genome step by step. First, SBJ1000::2*attB*, which harbours two artificial ΦC31 *attB* sites, was constructed by deleting the second non-target cluster, BGC3, based on SBJ1000::*attB*. Similarly, SBJ1000::3*attB* was generated from SBJ1000::2*attB* by replacing the third non-target cluster, BGC2, with an artificial ΦC31 *attB* site (Fig. 2a). Further deletion of the two non-target BGCs had no obvious effect on PII production (Fig. 2b) and mycelium formation in fermen-

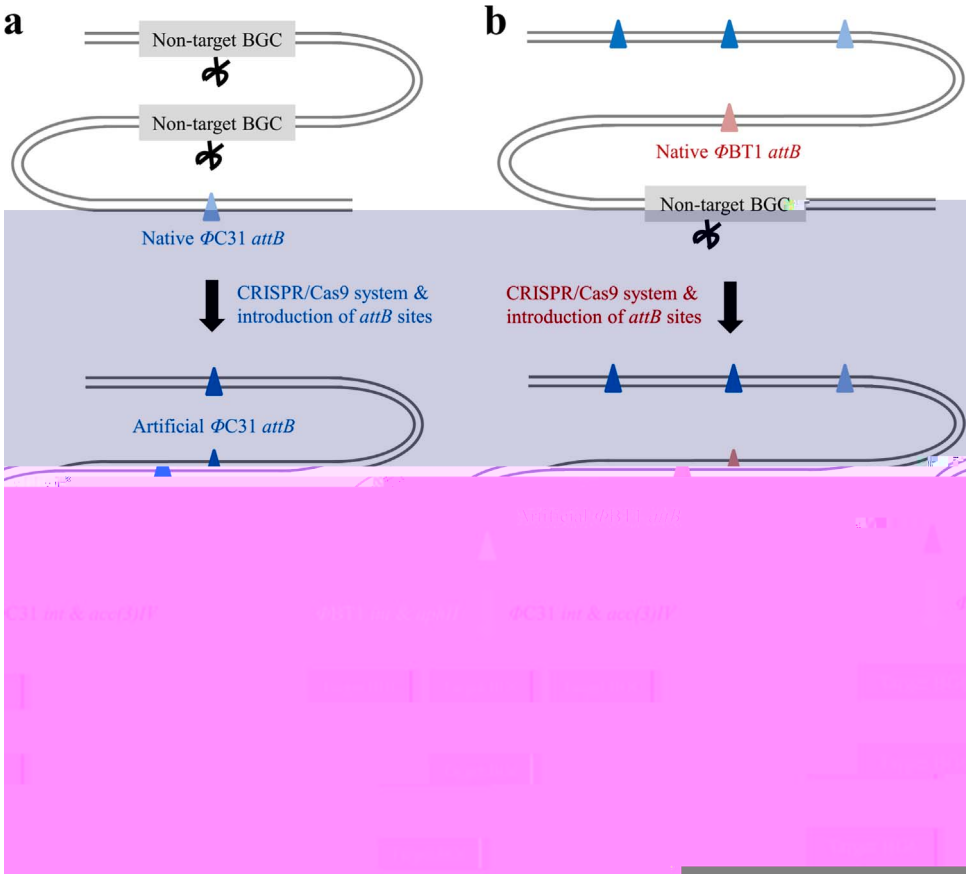

Fig. 1. Design principle of the MSGE method. (a) The ΦC31 Att/Int system enables the single-step, multi-copy chromosomal integration of target BGCs. Using the CRISPR/Cas9 genome editing method, artificial ΦC31 *attB* sites are inserted into the locations where the non-target BGCs were deleted. Light- and dark-blue triangles represent the native and artificial ΦC31 *attB* sites, respectively. (b) Two compatible Att/Int systems from phage ΦC31 and ΦBT1 are applied to the two-round amplification of target BGCs. After the artificial ΦBT1 *attB* sites are inserted into the modified genome harbouring multiple ΦC31 *attB* sites, target BGCs with different integration-resistance cassettes, ΦC31 *int* & *acc(3)IV* or ΦBT1 *int* & *aphII*, are integrated step-by-step into the corresponding *attB* sites. Light- and dark-red triangles represent the native and artificial ΦBT1 *attB* sites, respectively.

tation medium (data not shown). We found that when BAC-F1F15 was introduced into SBJ1000::2*attB*, only one of ten exconjugants contained three extra copies of the PII BGC, yielding SBJ1003 (Fig. S4b). However, we failed to obtain an engineered strain carrying four chromosomally integrated copies of the PII BGC when BAC-F1F15 was introduced into SBJ1000::3*attB* (Fig. S4c). These results indicated that the integration efficiency continuously declines as more copies of the PII BGC are introduced by the MSGE method.

We found that SBJ1002 and SBJ1003 exhibited no obvious growth difference on solid agar plates compared with SBJ1000 and SBJ1001 (Fig. S51). Importantly, the maximum PII production of SBJ1003 reached approximately 720 mg/L, representing 34% and 125% improvements over SBJ1002 and SBJ1000, respectively (Fig. 2c). The addition of 6% macroreticular resin HB60, which can absorb pristinamycin *in situ* and thereby weaken its toxic effect and feedback inhibition (Jia et al., 2006), further increased the PII titers of SBJ1003 to 1.78 g/L, which were 16% and 150% higher than those of SBJ1002 and SBJ1000, respectively (Fig. 2d). Finally, qRT-PCR analysis was performed to examine the effects of BGC amplification at the transcriptional level. Four PII biosynthetic genes, *snaE3*, *snaF*, *snaG* and *snaN*, were selected and tested. Consistent with the elevated PII titers following BGC amplification, the expression levels of these genes increased in step with increasing copy numbers of the PII BGC at early stages of fermentation (22 h) (Fig. S6a). However, although SBJ1002 and SBJ1003 produced higher PII titers than SBJ1000, all of the tested genes in these two engineered strains exhibited similar and even slightly reduced transcription compared with that in SBJ1000 after 30 h and 48 h of fermentation, respectively (Fig. S6a). This phenomenon may be due to product inhibition of pristinamycin biosynthesis as described previously (Jia et al., 2006). Growth analysis by light microscopy also revealed that, compared with the parental strain SBJ1000, which showed normal mycelium formation, SBJ1002 and SBJ1003 formed sparse, short mycelia after 72 h of fermentation (Fig. S6b). This phenomenon may be ascribed to the toxic effects of higher PII production on mycelium formation upon multi-copy PII BGC integration. Overall, MSGE via the 'one integrase-multiple *attB* sites' concept achieved the single-step, three-copy chromosomal integration of the PII BGC, which significantly improved PII production in *S. pristinaespiralis*.

3.3. Employing MSGE for second-round amplification of the PII BGC in S. pristinaespiralis

To explore whether PII production could be further enhanced by integrating more copies of the PII BGC into the *S. pristinaespiralis* chromosome, we employed MSGE again for second-round BGC amplification based on the compatible ΦBT1 Att/Int system. The first step was to replace the ΦC31 integrase/*attP* and the apramycin resistance marker (ΦC31 *int* & *acc(3)IV* cassette) of the plasmid BAC-F1F15 by the ΦBT1 integrase/*attP* and the kanamycin resistance marker (ΦBT1 *int* & *aphII* cassette). To quickly achieve this, we developed a new *in vitro* DNA editing method by combining the CRISPR/Cas9 system with Gibson assembly (Gibson et al., 2009; Jinek et al., 2012), in which Gibson assembly was used to repair the Cas9-generated sticky ends and thus refactor DNA fragments. The plasmid BAC-F1F15 was digested with the RNA-guided Cas9 endonuclease at designated target sites to release the ΦC31 *int* & *acc(3)IV* cassette. Then, the ΦBT1 *int* & *aphII* cassette from plasmid pRT802 (Gregory

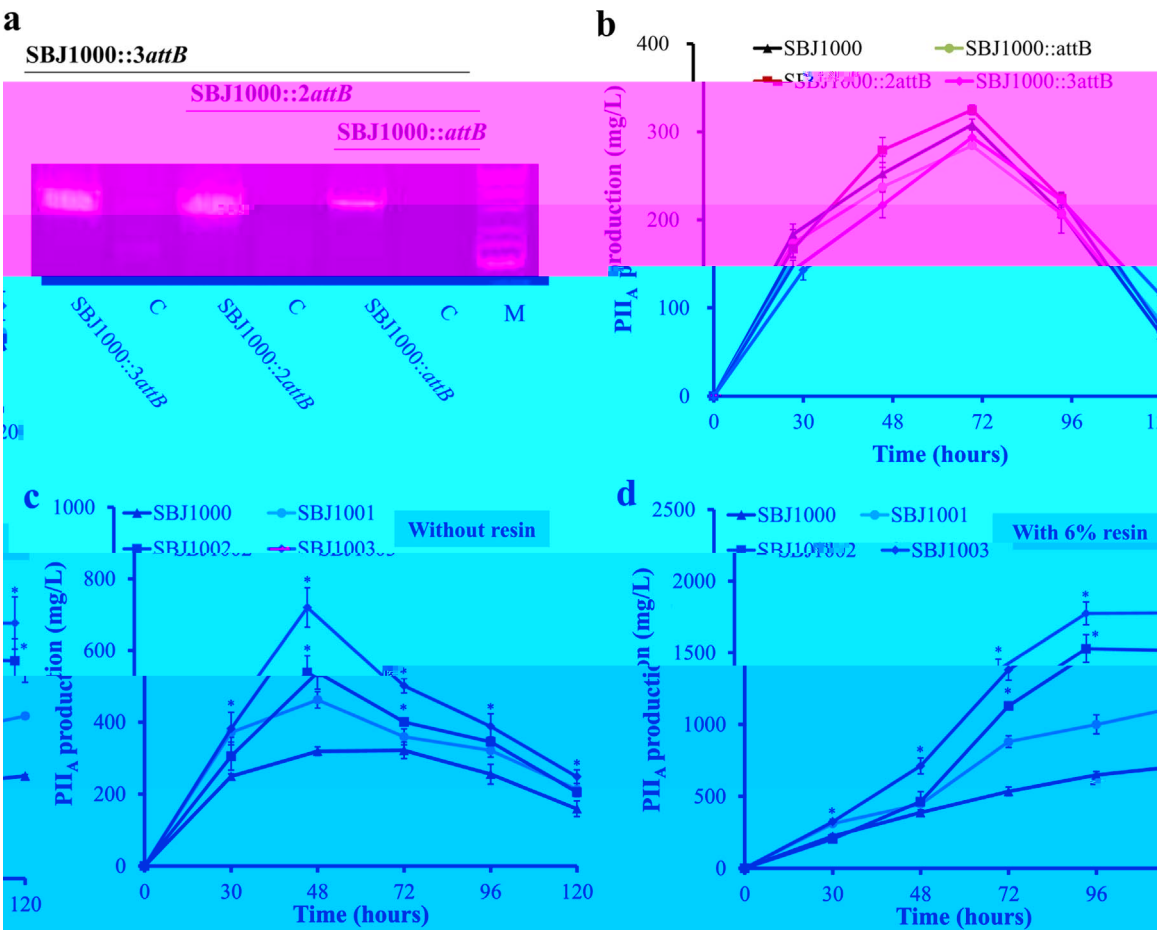

Fig. 2. MSGE improves PII production titers via the ΦC31 Att/Int system. Genetic (a) and fermentation analysis (b) of mutants with different numbers of artificial ΦC31 *attB* sites. C and M represent the starting strain SBJ1000 and the 1 kb DNA ladder (Thermo Scientific), respectively. PII_A production by the engineered strains (SBJ1000-SBJ1003) with zero to three extra copies of the PII BGC without resin HB60 (c) and with 6% (w/v) resin at 24 h after fermentation (d). The fermentation samples were collected at five time-points and the fermentations were performed in triplicate, $^*p < 0.05$.

et al., 2003) were ligated to the linearized plasmid BAC-F1F15 in a Gibson assembly mix to generate the recombinant plasmid BAC-F1F15(BT-*aphII*) (Fig. 3a and b). By restriction and DNA sequencing analysis, we found that this new DNA editing method could rapidly execute the replacement of the integration-resistance cassette with 45% efficiency (Fig. 3c).

Next, the recombinant plasmid BAC-F1F15(BT-*aphII*) was introduced into SBJ1003 containing a native ΦBT1 *attB* site to generate SBJ1004. Considering that the SBJ1003 genome contains a total of four copies of the PII BGC, homologous recombination (HR) may occur following the introduction of BAC-F1F15(BT-*aphII*). Therefore, we compared the frequency of HR and site-specific recombination (SSR) and showed that the plasmid BAC-F1F15(BT-*aphII*) could be integrated into the chromosome by SSR with 90% efficiency (Fig. S7a**)**. In fact, the nature of SSR, namely, that the recombination process requires cleavage of the genome, theoretically ensures a higher frequency of integration into the host chromosome than that of HR for a given *Streptomyces* strain. Upon addition of 6% resin HB60, the PII titer of SBJ1004 further reached 2.06 g/L after 96 h of fermentation, representing a 16% improvement over SBJ1003 (Fig. 4).

To assess whether the PII BGC could be further amplified by the MSGE method, we introduced an artificial ΦBT1 *attB* site into SBJ1000::2*attB* following deletion of the non-target cluster BGC15, yielding SBJ1000::2*attB*::*attBT*. Similarly, SBJ1000::2*attB*::2*attBT* was also constructed by inserting a second artificial ΦBT1 *attB* site into the deleted cluster BGC5 (Fig. 4a). Deleting the two non-target BGCs had no obvious effect on PII production (Fig. 4b) and mycelium formation in fermentation medium (data not shown). Then, we introduced BAC-F1F15 into SBJ1000::2*attB*::*attBT* and SBJ1000::2*attB*::2*attBT* via the ΦC31 Att/Int system for first-round amplification of the PII BGC, generating SBJ1003::*attBT* and SBJ1003::2*attBT*, respectively. Fermentation analysis showed that the two intermediate strains produced PII titers similar to those of SBJ1003 (data not shown). Subsequently, BAC-F1F15(BT-*aphII*) was transferred into SBJ1003::*attBT*, and 90% of the exconjugants exhibited simultaneous chromosomal integration of two copies of BAC-F1F15(BT-*aphII*), generating SBJ1005 (Fig. S7b). However, we failed to obtain an engineered strain containing six extra copies of the PII BGC due to the absence of exconjugants following the introduction of BAC-F1F15(BT-*aphII*) into SBJ1003::2*attBT*. On solid RP agar plates, we found that SBJ1005 exhibited no obvious growth difference compared with SBJ1004 and SBJ1003 (Fig. S8).

Finally, we evaluated whether the introduction of a fifth extra copy of the PII BGC enhanced PII production. Fermentation analysis showed that the final engineered strain SBJ1005 containing five extra copies of the PII BGC produced a PII titer of 2.24 g/L upon addition of 6% resin HB60, which was 9% and 216% higher than SBJ1004 and the starting strain SBJ1000, respectively (Fig. 4c). However, without the presence of resin in the fermentation medium, SBJ1004 and SBJ1005 produced lower PII titers than SBJ1003 (Fig. S9a). Growth analysis revealed that during the early stage of fermentation (48 h), SBJ1004 and SBJ1005 formed short, sparse mycelia compared with SBJ1003, which showed normal mycelium formation (Fig. S9b). Therefore, we speculated that further integration of the PII BGC in SBJ1003 might result in precocious and higher transcription of the PII biosynthetic genes and thus disrupt normal bacterial growth at early stages of

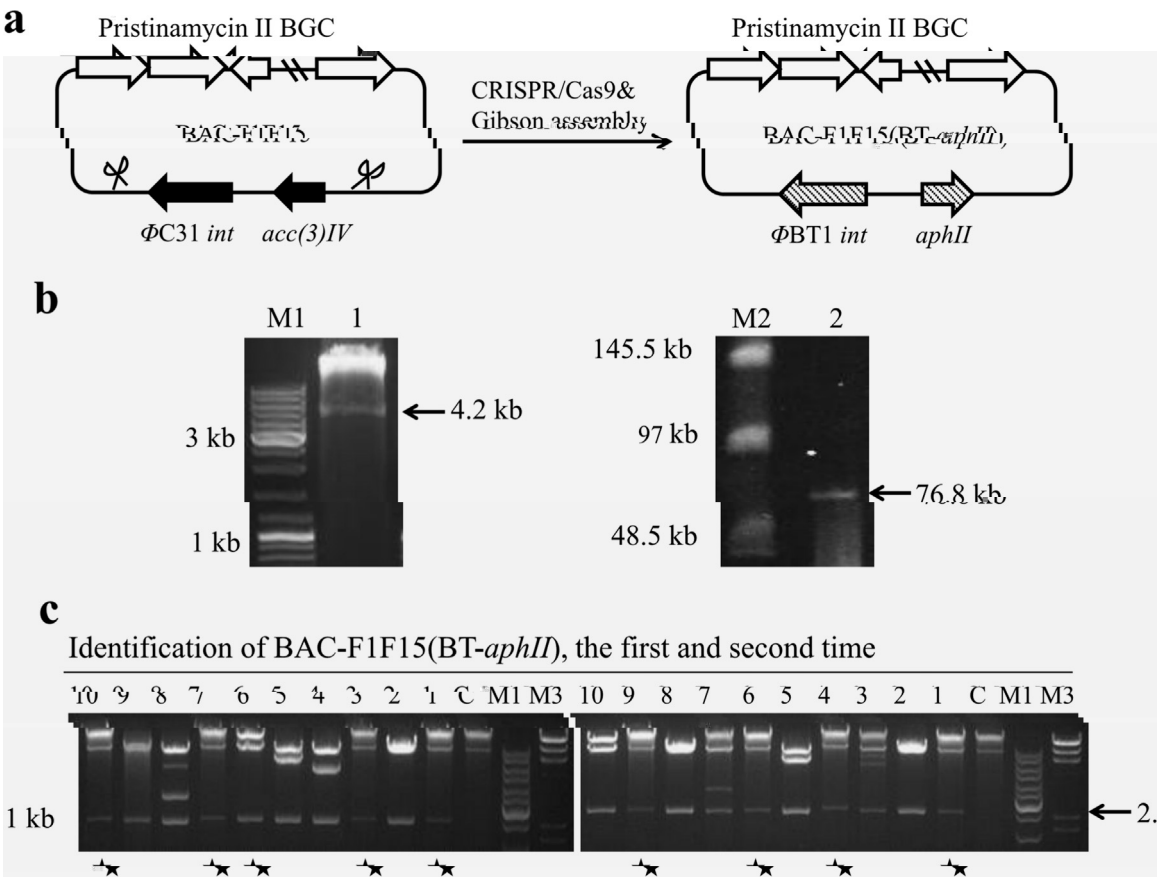

Fig. 3. *In vitro* DNA editing by combining the CRISRP/Cas9 system with Gibson assembly. (a) Schematic representation of this DNA editing method used to replace the integration-resistance cassette. The plasmid BAC-F1F15 is cleaved by the RNA-guided Cas9 endonuclease at the designated sites to release the *Φ*C31 *int* & *acc(3)IV* cassette, and the *Φ*BT1 *int* & *aphII* cassette is then ligated to the digested plasmid in a Gibson assembly mix. (b) Analysis of the plasmid BAC-F1F15 (81 kb) after digestion using the Cas9 endonuclease by agarose gel electrophoresis (left) and PFGE (right). 1 and 2 represent the *Φ*C31 *int* & *acc(3)IV* cassette (4.2 kb) and the digested plasmid (76.8 kb), respectively. M1 and M2 represent the 1 kb DNA ladder and the λ PFG ladder (NEB), respectively. (c) *Nhe* I restriction analysis of the recombinant plasmid BAC-F1F15(BT-*aphII*). M3 represents the λ *Hin*d III DNA ladder (Takara). Asterisks (★) indicate correct DNA assembly.

fermentation. This incoordination might ultimately lead to the lower PII titers in SBJ1004 and SBJ1005. Furthermore, the end-product feedback effect may become stronger after introduction of more copies of the PII BGC, thus resulting in tighter repressive effects on PII biosynthesis in SBJ1004 and SBJ1005. Nevertheless, we demonstrated that the compatible *Φ*BT1 Att/Int system could be employed for the second-round amplification of the PII BGC by the MSGE method and further enhancing PII production in *S. pristinaespiralis*.

3.4. *Validation of genetic stability and fermentation scale-up in* S. pristinaespiralis

To examine the genetic stability of engineered strains constructed by MSGE, SBJ1003 and SBJ1005 were cultured over five generations in the absence of antibiotic selection. Fermentation analysis showed that the first (G1), third (G3) and fifth (G5) generations of SBJ1003 or SBJ1005 were capable of producing PII titers that were similar to their corresponding starting strains (Fig. 5a and b). Furthermore, genetic analysis by PCR also indicated that all of the PII BGCs amplified by MSGE were stably maintained in the two high-producing strains (Fig. S10). Subsequently, we tested the scale-up feasibility of these integrated PII BGCs by batch fermentation in a 5-L bioreactor. The results showed that upon addition of 6% resin HB60, SBJ1003 and SBJ1005 accumulated a maximum PII level of 1.67 and 2.02 g/L after 96 h of fermentation, showing a 1.7- and 2.3-fold improvement, respectively, over the parental strain SBJ1000 (Fig. 5c). Overall, we confirmed that MSGE achieved the stable, higher-order amplification of the PII BGC, which is valuable for robust genome engineering of other industrial actinomycetes.

3.5. *Extending MSGE to develop powerful* S. coelicolor *heterologous hosts*

Along with the emergence of genome mining as a robust approach to discover novel natural products, the development of reliable heterologous hosts to express cryptic/silent secondary metabolite BGCs is becoming increasingly important (Baltz, 2010; Ongley et al., 2013). On the basis of the wild-type strain *S. coelicolor* M145, M1146 and M1152 have been developed, which contained deletions in four active BGCs, responsible for the biosynthesis of actinorhodin (ACT), prodiginine (RED), cryptic type I polyketides (CPK) and calcium-dependent antibiotic (CDA), either alone or in combination with a point mutation in *rpoB*. The two engineered strains have been proven to be robust heterologous hosts for the expression of diverse secondary metabolite BGCs (Gomez-Escribano and Bibb, 2011, 2014). Here, we intended to construct a series of more powerful *S. coelicolor* heterologous hosts by introducing multiple *Φ*C31 *attB* sites into the genome of M1146 and M1152 (Fig. 6a). As such, these special hosts, with the original simplified metabolic profiles of M1146 or M1152, could potentially be used to achieve higher titers of bioactive secondary metabolites by single-step, multi-copy chromosomal integration of cloned BGCs.

We first inserted an artificial *Φ*C31 *attB* site into the location where the CPK BGC was deleted in M1146 and M1152 using the highly-efficient CRISPR/Cas9 genome editing method, generating M1246 and M1252, respectively. Similarly, M1346-M1546 (based on M1146,

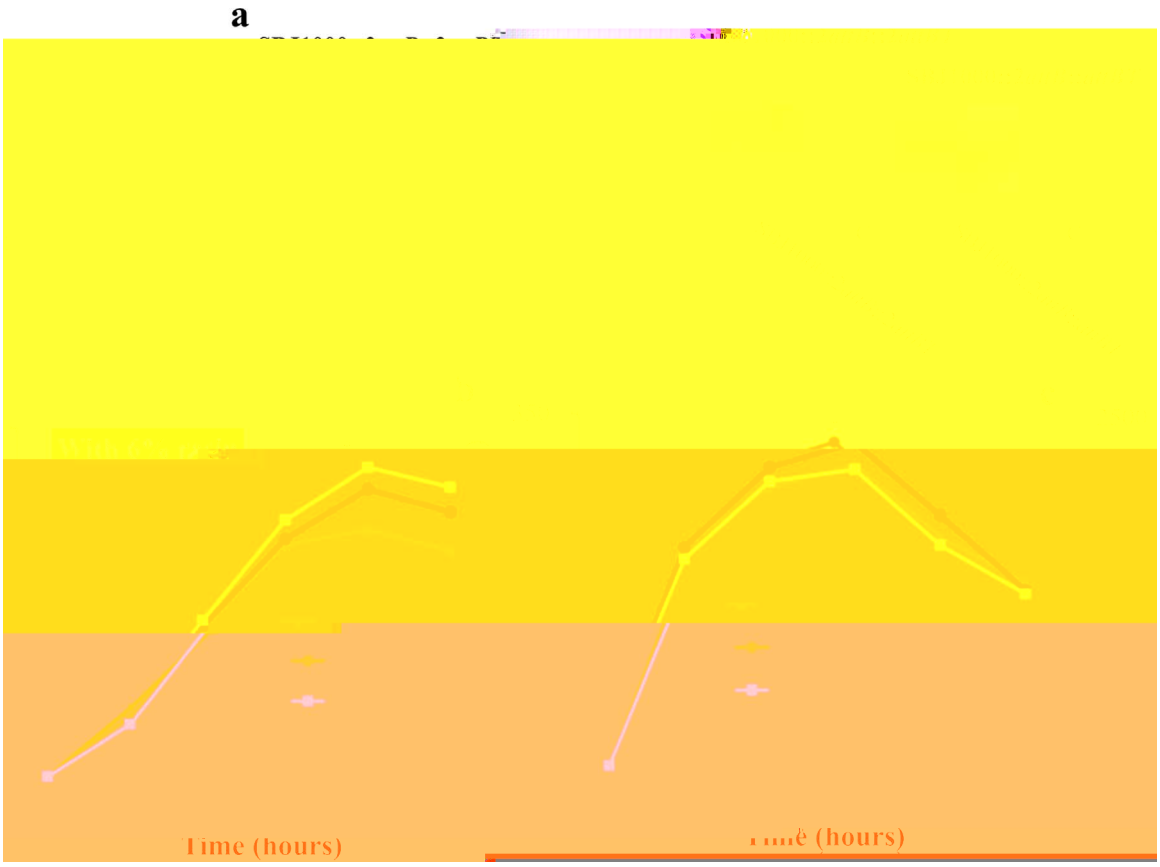

Fig. 4. MSGE further improves PII production titers by combining two compatible Att/Int systems. Genetic (a) and fermentation analysis (b) of mutants with different numbers of artificial *Φ*BT1 *attB* sites. C and M represent the starting strain SBJ1000::2*attB* and the 1 kb DNA ladder, respectively. (c) PII_A production by the engineered strains (SBJ1003-SBJ1005) with three to five extra copies of the PII BGC. 6% (w/v) resin HB60 was added at 24 h after fermentation. The fermentation samples were collected at five time-points and the fermentations were performed in triplicate, $^*p < 0.05$.

containing two to four artificial *Φ*C31 *attB* sites) and M1352-M1552 (based on M1152, containing two to four artificial *Φ*C31 *attB* sites) were constructed by the step-by-step introduction of *Φ*C31 *attB* sites into the three respective locations where the RED, CDA and ACT BGCs were deleted. All of the resulting strains were verified by PCR and sequence analysis (Fig. 6b). Growth analysis revealed that M1246-M1546 and M1252-M1552 sporulated well as the parental strain M1146 and M1152, respectively (data not shown).

To assess the performance of the engineered strains for heterologous expression, the chloramphenicol BGC (cloned in the cosmid pAH91) from *Streptomyces venezuelae* and the anti-tumour compound YM-216391 BGC (cloned in the cosmid pST85) from *Streptomyces nobilis* were introduced into M1152-M1552 and M1146-M1546, respectively, by a single round of conjugal transfer (Fig. 7a) (Gomez-Escribano and Bibb, 2011; Jian et al., 2012). Considering that M1146 produced 10 times less chloramphenicol than M1152 in a previous study (Gomez-Escribano and Bibb, 2011), M1146 and its derivatives (M1246-M1446) were not used for heterologous expression of the chloramphenicol BGC. We found that the chloramphenicol and YM-216391 BGCs were integrated into all of the *Φ*C31 *attB* sites in M1152 and its derivatives (M1252-M1452) with almost 100% efficiency (Fig. S11 and S12). Similarly, the YM-216391 BGC was efficiently integrated into M1146 and its derivatives (M1246-M1446) (data not shown). However, using M1552 or M1546 as the recipient strains yielded no exconjugants. In fact, we also found that only a dozen exconjugants were obtained when pAH91 was introduced into M1452 or when pST85 was introduced into M1452 and M1446 (data not shown). Furthermore, with the increasing copy numbers of the chloramphenicol or YM-216391 BGCs, the growth of these engineered strains was getting worse on MS agar plates (Fig. S13). These results suggested that high-order amplification of BGCs or the accumulation of target products placed an excess burden on bacterial growth.

Subsequently, the titers of chloramphenicol and YM-216391 were determined by HPLC analysis. The fermentation results showed that the production of both chloramphenicol and YM-216391 was significantly enhanced with increasing copy numbers of the corresponding BGCs (Fig. 7b). M1452/pAH91 produced 2 times chloramphenicol than M1152/pAH91 (from 36.3 mg/L to 110.4 mg/L). However, M1452/pAH91 exhibited only a very slight improvement in chloramphenicol production compared with M1352/pAH91 (from 104.6 mg/L to 110.4 mg/L) (Fig. 7b), suggesting that the expression of the chloramphenicol biosynthetic genes in M1352/pAH91 was no longer the bottleneck for antibiotic production. Further improvement of chloramphenicol production would require to consider other metabolic engineering strategies, such as increasing precursor availability and enhancing antibiotic tolerance. Regarding the production of YM-216391, the two engineered strains M1452/pST85 and M1446/pST85 exhibited maximum production increases of 10.2- (from 3.3 to 36.4 mg/L) and 22.8-fold (from 0.5 to 12.1 mg/L) compared with M1152/pST85 and M1146/pST85, respectively (Fig. 7b and S14a). Notably, M1452/pST85, which carries a point mutation [S433L] in *rpoB* (encoding the RNA polymerase β-subunit), produced 2 times YM-216391 than M1446/pST85 (Fig. 7b and S14a). This phenomenon was consistent with the previous reported effects of the point mutations (conferring resistance to rifampicin) in *rpoB*, which resulted in secondary metabolite overproduction in actinomycetes (Gomez-Escribano and Bibb, 2011; Tanaka et al., 2013).

Finally, we performed qRT-PCR analysis to examine the effects of BGC amplification at the transcriptional level. Four chloramphenicol biosynthetic genes (*cmlC*, *cmlK*, *cmlP* and *cmlR*) and four YM-216391

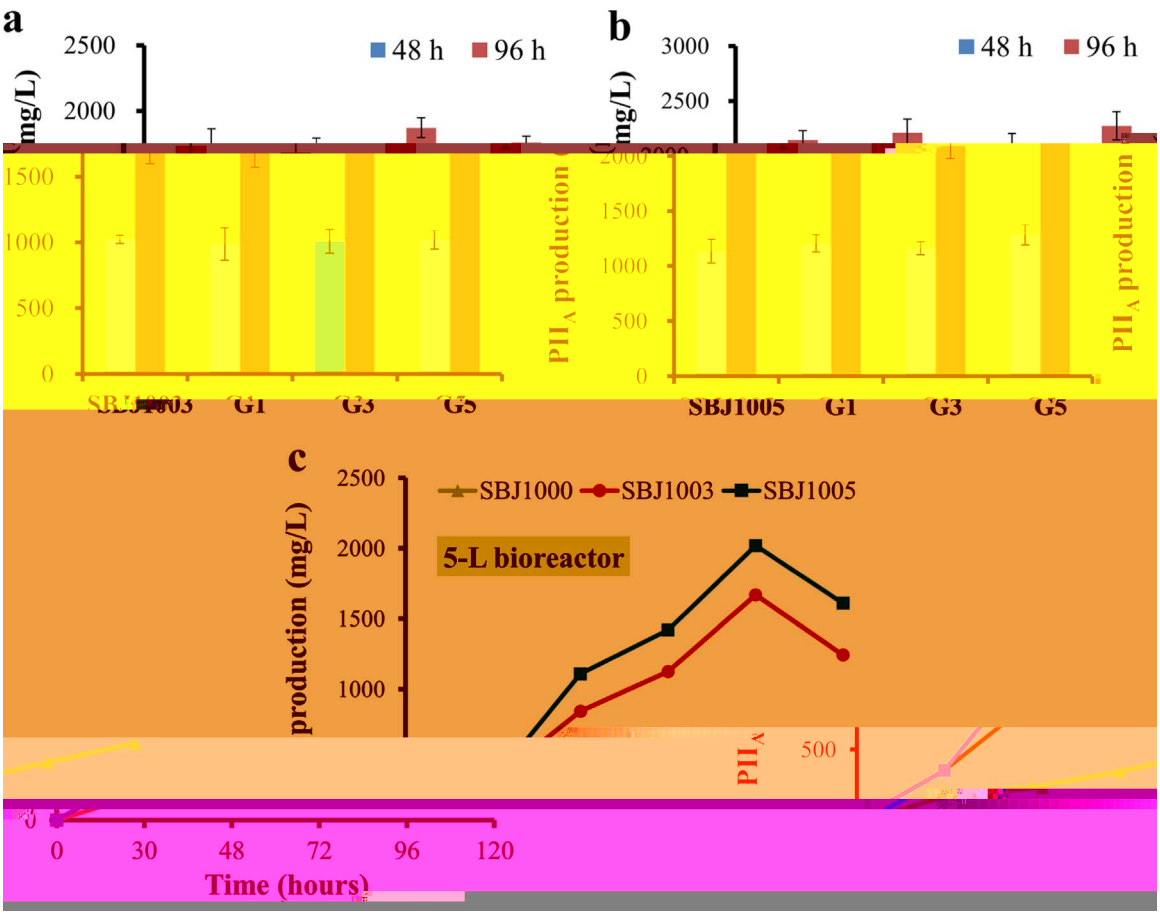

Fig. 5. Genetic stability and scale-up fermentation of SBJ1003 and SBJ1005. Fermentation analysis of the first (G1), third (G3) and fifth (G5) generations of SBJ1003 (a) and SBJ1005 (b) over five successive sub-cultivation in the absence of antibiotic selection. The fermentation samples were collected at 48 h and 96 h and the fermentations were performed in triplicate. (c) PII_A production by SBJ1003 and SBJ1005 compared with the parental strain SBJ1000 in a 5-L bioreactor. The fermentation samples were collected at five time-points. For all experiments, 6% (w/v) resin HB60 was added at 24 h after fermentation.

biosynthetic genes (*ymA*, *ymB1*, *ymBC* and *ymR4*) were tested and *hrdB*, which encodes the major vegetative sigma factor, was used as an internal control (Gomez-Escribano and Bibb, 2011; Jian et al., 2012). RNA samples were isolated from fermentation cultures of all recombinant strains at 2 and 4 days. Overall, chloramphenicol biosynthetic gene expression gradually increased with BGC amplification, which was largely consistent with the phenotypic changes in chloramphenicol production (Fig. 7c). A similar phenomenon was also detected for YM-216361 biosynthetic gene expression, with M1452/pST85 and M1446/pST85 showing the highest mRNA levels at both tested time points (Fig. 7c and S14b). These results suggested that BGC amplification increased biosynthetic gene expression and thereby facilitated the biosynthesis of the target products.

4. Discussion

Effective tools to optimize the biosynthetic performance of microbial secondary metabolites are essential to solve early-stage discovery and late-stage cost-efficient production problems, and the development of such tools has remained a long-standing challenge (Baltz, 2016b; Weber et al., 2015b; Zhang et al., 2016). In this study, we describe a potentially general metabolic engineering approach, MSGE, based on site-specific recombination to modify actinomycetes for the high-level production of bioactive small molecules by single-step, multi-copy chromosomal integration of target BGCs.

To promote the industrial-scale production of pristinamycin, MSGE was employed for the stable amplification of the PII BGC based on our prior optimized strain SBJ1000 (Li et al., 2015). We demonstrated that two compatible Att/Int systems from phages *Φ*C31 and *Φ*BT1 were capable of successively achieving three- and two-copy chromosomal integration of the PII BGC. Upon addition of 6% resin HB60, the final strain SBJ1005, carrying five extra copies of the PII BGC, produced PII titers of 2.24 and 2.02 g/L under flask- and batch-fermentation conditions, respectively. To the best of our knowledge, these are the highest titers reported to date. Furthermore, compared with the tandem amplification of target BGCs by the ZouA-mediated DNA recombination system, which may be unstable without antibiotic selection (Murakami et al., 2011), all of the amplified PII BGCs were stably maintained over five successive sub-cultivation tests, highlighting the genetic stability of these high-producing strains constructed by MSGE. This property ensured the steady production performance of the engineered actinomycetes strains in large-scale fermentation. In fact, the unidirectional nature of site-specific recombination and the discrete distribution of the amplified BGCs theoretically ensure the generation of stable exconjugants. We believe that this simple and efficient amplification platform will markedly facilitate the robust genome engineering of other important industrial actinomycetes (Baltz, 2016b).

With the emergence of genome mining as a general approach to discover novel bioactive secondary metabolites, it is very critical to develop reliable and versatile *Streptomyces* species and other actinomycetes hosts for high-level heterologous expression of cryptic BGCs (Baltz, 2010, 2016b). In the present study, MSGE was successfully extended to construct a series of powerful heterologous hosts with different numbers of *Φ*C31 *attB* sites based on *S. coelicolor* M1146 or M1152, which possess simple metabolite profiles combined with ease

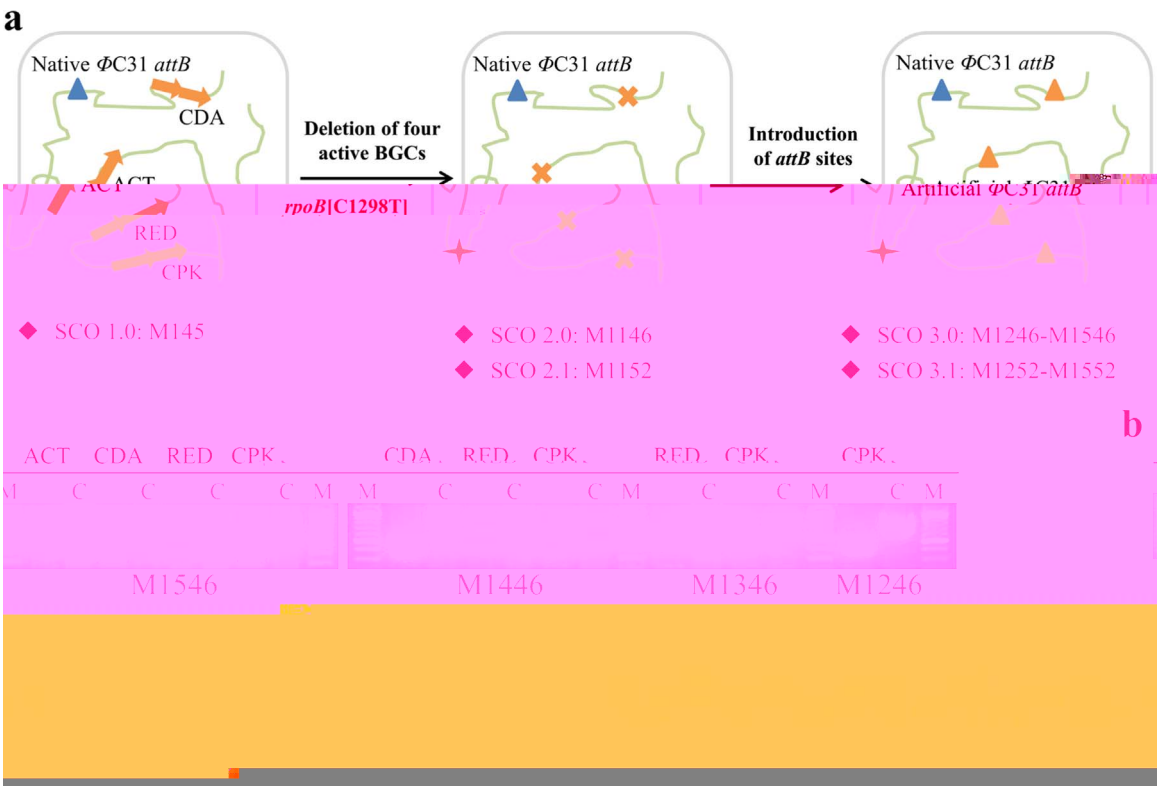

Fig. 6. Design and construction of the *Streptomyces coelicolor* heterologous hosts. (a) Design principle employed for a panel of powerful heterologous hosts by step-by-step insertion of artificial ΦC31 *attB* sites into the locations where the four known secondary metabolite BGCs were deleted in *S. coelicolor* M1146 and M1152. Yellow arrows represent the active ACT, RED, CDA and CPK BGCs. Blue and yellow triangles represent the native and artificial ΦC31 *attB* sites, respectively. The red asterisk indicates the point mutation in *rpoB*. (b) Genetic analysis of the *S. coelicolor* mutants M1246-M1546 and M1252-M1552. C represents M1146 or M1152. M represents the 1 kb DNA ladder.

of culturing and genetic manipulation (Gomez-Escribano and Bibb, 2011). Up to four copies of the chloramphenicol and YM-216391 BGCs could be efficiently integrated into *S. coelicolor* chromosome in a single step, resulting in significantly enhanced productivity (2–23 times). We observed a clear correlation between BGC copy number and the production levels of target products. Additionally, we noticed that the engineered strains carrying multiple copies of the chloramphenicol or YM-216391 BGCs exhibited increasingly weak growth on solid agar plates, potentially due to the toxic effects of antibiotic overproduction. To guarantee efficient biosynthesis of target products, we suggest that sufficient mycelia should be cultivated on solid MS medium before being transferred into liquid seed medium. We expect that the engineered *S. coelicolor* heterologous hosts will markedly facilitate the discovery of novel natural products as well as the yield improvement of important clinically used drugs from genetically inaccessible actinomycetes (Baltz, 2016b; Zhang et al., 2016).

When our work was drawing to a close, a similar approach for amplifying target BGCs was published in *Streptomyces albus* J1074 (Manderscheid et al., 2016). Inspired by the presence of two highly active ΦC31 *attB* sites in *S. albus* J1074, Manderscheid and coworkers further introduced an artificial ΦC31 *attB* site into the chromosome via transposon mutagenesis (Bilyk and Luzhetskyy, 2014). The resulting host, carrying a total of three ΦC31 *attB* sites, was successfully employed to overproduce four different antibiotics. However, it is worth noting that the engineered strains carrying three integrated copies of the cloned BGCs exhibited large fluctuations in antibiotic production due to the unstable insertion of the artificial ΦC31 *attB* site. Considering *S. albus* J1074 as another well-characterized heterologous host (Baltz, 2016b; Iqbal et al., 2016), we are now using MSGE to develop a panel of more stable *S. albus* strains. Furthermore, MSGE can also be applied to other promising actinomycetes hosts, such as *Streptomyces avermitilis* and *Saccharopolyspora erythraea* (Baltz, 2010).

The actinomycetes genome can encode a large number of BGCs, ranging from 5 to 52 (average of 27.4) per genome, which serve as an untapped reservoir for the discovery of novel pharmaceutically active compounds (Baltz, 2016a). Here we demonstrate a new way to take advantage of these cryptic BGCs as deletion/integration sites. More importantly, we systematically observed the integration efficiency when different copy numbers of various BGCs were introduced into *S. pristinaespiralis* and *S. coelicolor* (Table 1). We demonstrated that the genomic locations of *attB* sites play an important role in the efficiency of the multi-copy integration of target BGCs (Fig. S15). We showed that although *S. coelicolor* and *S. pristinaespiralis* exhibit similar transconjugant frequencies (Baltz, 2012), the former was capable of integrating four copies of the PII BGC with almost 100% efficiency, whereas the latter achieved three-copy integration with only 10% efficiency (Fig. S4 and S16). Furthermore, neither the PII nor chloramphenicol BGC could be simultaneously inserted with four copies into *S. pristinaespiralis*, potentially due to the existence of two adjacent *attB* sites (Fig. S4 and S17). These results indicate that the discrete distributions of *attB* sites in the chromosome are essential to guarantee a high integration efficiency by the MSGE method. In addition, the efficiency is likely to be affected by other factors, e.g., the plasmid copy number. Compared with the triplication of the PII BGC (cloned in the single-copy BAC-F1F15) at an efficiency of 10%, we showed that three copies of the chloramphenicol BGC (cloned in the multi-copy cosmid pAH91) could be integrated into *S. pristinaespiralis* with 85% efficiency (Fig. S4 and S16). Nevertheless, the powerful *S. coelicolor* heterologous hosts developed in this study are capable of integrating up to four copies of different BGCs with almost 100% efficiency, regardless of the copy number of recombinant plasmids containing the target BGCs (Table 1). This advantage will benefit functional metagenomics screening through the construction of cosmid or BAC libraries to unlock previously unexplored biosynthetic diversity (Katz et al., 2016).

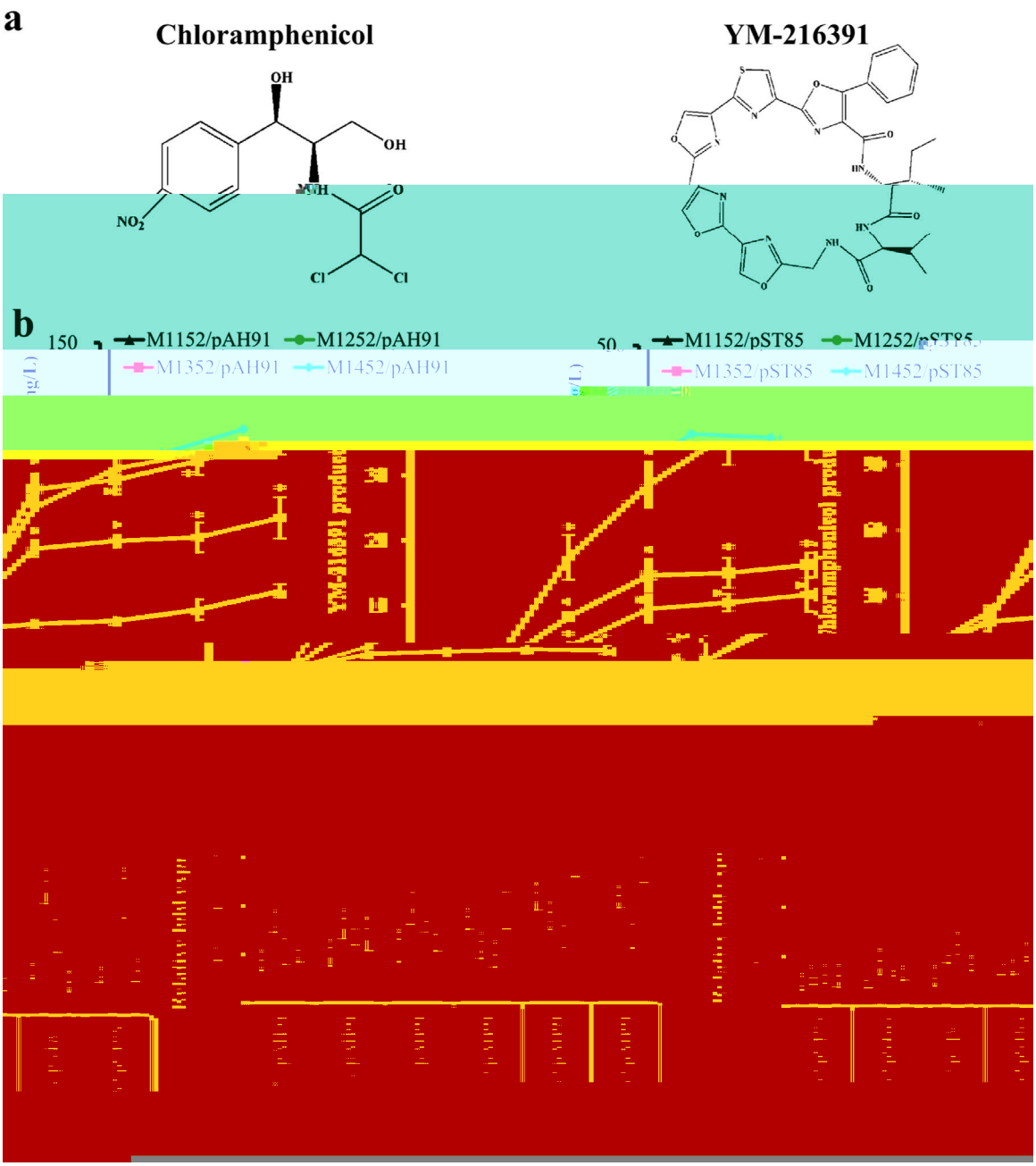

Fig. 7. Heterologous expression of the chloramphenicol and YM-216391 BGCs. (a) Chemical structures of the two bioactive secondary metabolites (antibiotic chloramphenicol and anti-tumour compound YM-216391) used in this study. (**b**) Fermentation analysis of the engineered strains with one to four copies of the chloramphenicol or YM-216391 BGCs. The fermentation samples were collected at five time-points and the fermentations were performed in triplicate, $^{*}p < 0.05$. (c) Transcriptional analysis of four selected chloramphenicol or YM-216391 biosynthetic genes. The fermentation samples for RNA isolation were collected at 2 and 4 days. The relative transcription levels of the tested genes were normalized to that of the *hrdB* gene. The relative fold-changes in the expression of each gene (M1252/pAH91-M1452/pAH91 versus M1152/pAH91 or M1252/pST85-M1452/pST85 versus M1152/pST85) were determined using the $2^{-\Delta\Delta Ct}$ method. Error bars indicate the standard deviations from three independent biological replicates, $^{*}p < 0.05$.

Table 1
Integration efficiency of different BGCs in *S. pristinaespiralis* and *S. coelicolor*.

S. pristinaespiralis	**BAC-F1F15** (81 kb)	**pAH91** (~40 kb)	***S. coelicolor***	**pAH91** (~40 kb)	**pST85** (~35 kb)	**BAC-F1F15** (81 kb)
SBJ1000::*attB*	100% (10/10+10/10)	95% (9/10+10/10)	M1252	100% (10/10+10/10)	95% (10/10+9/10)	95% (9/10+10/10)
SBJ1000::2*attB*	10% (1/10+1/10)	85% (9/10+8/10)	M1352	100% (10/10+10/10)	100% (10/10+10/10)	100% (10/10+10/10)
SBJ1000::3*attB*	0% (0/10+0/10)	0% (0/10+0/10)	M1452	80% (8/10+8/10)	85% (7/10+10/10)	85% (8/10+9/10)
			M1552	ND	ND	ND

All experiments were performed in duplicate. ND: not detected due to the absence of exconjugants when the three plasmids were introduced into M1552.
BAC-F1F15, pAH91 and pST85 contain the BGCs for the biosynthesis of pristinamycin II, chloramphenicol and YM-216391, respectively.

In the past, the concept of combining the *in vitro* CRISPR/Cas9 system with Gibson assembly has been applied to the seamless cloning of a single gene or large gene clusters (up to 100 kb) (Jiang et al., 2015a; Wang et al., 2015). Here, a new *in vitro* DNA editing method was established via the same concept to rapidly introduce the *Φ*BT1 Att/Int system for second-round amplification of the PII BGC. In constrast to other DNA editing methods based on homologous recombination in *Saccharomyces cerevisiae*, such as DNA assembler (Shao et al., 2011) and mCRISTAR (Kang et al., 2016), this new method requires only 2–3 days and thus simplifies efforts to refactor target BGCs. To demonstrate the generality of this DNA editing method, we modified the transcriptional activator gene *cmlR* within the chloramphenicol BGC by replacing the native promoter with the strong promoter *kasO*p*(Wang et al., 2013b) and by performing in-frame deletion, respectively (Fig. S18a). We showed that, without the aid of the resistance marker, this new method seamlessly catalyzed targeted editing with a positive rate of 25%, including in-frame deletion of single gene(s) and exchange of promoters (Fig. S18b). Consistent with a previous report (Fernandez-Martinez et al., 2014), deletion of the cluster-situated activator gene *cmlR* blocked chloramphenicol production and *cmlR* overexpression increased chloramphenicol production (Fig. S18c). Importantly, in contrast to the ICE system obtained by combining the *in vitro* CRISPR/Cas9 system and T4 DNA polymerase (Liu et al., 2015), our new DNA editing method does not generate frame-shift mutations, which is particularly valuable for precise combinatorial biosynthesis (Kim et al., 2015). Collectively, our development of *S. coelicolor* expression hosts, coupled with this new DNA editing method, should promote natural product research, including pathway identification, combinatorial biosynthesis and the activation of silent BGCs (Kim et al., 2015; Rutledge and Challis (2015); Smanski et al., 2016).

In conclusion, MSGE for single-step, site-specific, multi-copy chromosomal integration of target BGCs provides a simple and general metabolic engineering approach with broad applicability, mainly including the following two fields: (1) engineering industrial actinomycetes for large-scale manufacturing (Olano et al., 2008; Zhang et al., 2016); (2) developing reliable expression hosts for discovering and developing novel bioactive secondary metabolites from actinomycetes (Baltz, 2010, 2016b).

Acknowledgements

We thank Professor Mervyn Bibb (John Innes Centre, UK) for kindly providing the plasmid pAH91 and *Streptomyces coelicolor* M1146 and M1152. We also thank Professors Gongli Tang (Shanghai Institute of Organic Chemistry, CAS, China) and Xiaoming Ding (Fudan University, China) for kindly providing the plasmids pST85 and pRT802, respectively. This work was supported by National Natural Science Foundation of China (31421061, 31630003, 31430004, 31370081, 31570072) and the National Basic Research Program of China (2012CB721103).

Appendix A. Supporting information

Supplementary data associated with this article can be found in the online version at http://dx.doi.org/10.1016/j.ymben.2017.01.004.

References

Baltz, R.H., 2010. *Streptomyces* and *Saccharopolyspora* hosts for heterologous expression of secondary metabolite gene clusters. J. Ind. Microbiol. Biotechnol. 37, 759–772.

Baltz, R.H., 2012. *Streptomyces* temperate bacteriophage integration systems for stable genetic engineering of actinomycetes (and other organisms). J. Ind. Microbiol. Biotechnol. 39, 661–672.

Baltz, R.H., 2016a. Gifted microbes for genome mining and natural product discovery. J. Ind. Microbiol. Biotechnol. http://dx.doi.org/10.1007/s10295-016-1815-x.

Baltz, R.H., 2016b. Genetic manipulation of secondary metabolite biosynthesis for improved production in *Streptomyces* and other actinomycetes. J. Ind. Microbiol. Biotechnol. 43, 343–370.

Barka, E.A., Vatsa, P., Sanchez, L., Gaveau-Vaillant, N., Jacquard, C., Klenk, H.P., Clement, C., Ouhdouch, Y., van Wezel, G.P., 2015. Taxonomy, physiology, and natural products of actinobacteria. Microbiol. Mol. Biol. Rev. 80, 1–43.

Bilyk, B., Luzhetskyy, A., 2014. Unusual site-specific DNA integration into the highly active pseudo-*attB* of the *Streptomyces albus* J1074 genome. Appl. Microbiol. Biotechnol. 98, 5095–5104.

Cimermancic, P., Medema, M.H., Claesen, J., Kurita, K., Brown, L.C.W., Mavrommatis, K., Pati, A., Godfrey, P.A., Koehrsen, M., Clardy, J., Birren, B.W., Takano, E., Sali, A., Linington, R.G., Fischbach, M.A., 2014. Insights into secondary metabolism from a global analysis of prokaryotic biosynthetic gene clusters. Cell 158, 412–421.

Doroghazi, J.R., Albright, J.C., Goering, A.W., Ju, K.S., Haines, R.R., Tchalukov, K.A., Labeda, D.P., Kelleher, N.L., Metcalf, W.W., 2014. A roadmap for natural product discovery based on large-scale genomics and metabolomics. Nat. Chem. Biol. 10, 963–968.

Fernandez-Martinez, L.T., Borsetto, C., Gomez-Escribano, J.P., Bibb, M.J., Al-Bassam, M.M., Chandra, G., Bibb, M.J., 2014. New insights into chloramphenicol biosynthesis in *Streptomyces venezuelae* ATCC 10712. Antimicrob. Agents Ch. 58, 7441–7450.

Fierro, F., Barredo, J.L., Diez, B., Gutierrez, S., Fernandez, F.J., Martin, J.F., 1995. The penicillin gene-cluster is amplified in tandem repeats linked by conserved hexanucleotide sequences. Proc. Natl. Acad. Sci. 92, 6200–6204.

Gibson, D.G., Young, L., Chuang, R.-Y., Venter, J.C., Hutchison, C.A., Smith, H.O., 2009. Enzymatic assembly of DNA molecules up to several hundred kilobases. Nat. Methods 6, 343–345.

Gomez-Escribano, J.P., Bibb, M.J., 2011. Engineering *Streptomyces coelicolor* for heterologous expression of secondary metabolite gene clusters. Microb. Biotechnol. 4, 207–215.

Gomez-Escribano, J.P., Bibb, M.J., 2014. Heterologous expression of natural product biosynthetic gene clusters in *Streptomyces coelicolor*: from genome mining to manipulation of biosynthetic pathways. J. Ind. Microbiol. Biotechnol. 41, 425–431.

Gregory, M.A., Till, R., Smith, M.C., 2003. Integration site for *Streptomyces* phage phiBT1 and development of site-specific integrating vectors. J. Bacteriol. 185, 5320–5323.

Haginaka, K., Asamizu, S., Ozaki, T., Igarashi, Y., Furumai, T., Onaka, H., 2014. Genetic approaches to generate hyper-producing strains of goadsporin: the relationships between productivity and gene duplication in secondary metabolite biosynthesis. Biosci. Biotech. Bioch. 78, 394–399.

Harvey, A.L., Edrada-Ebel, R., Quinn, R.J., 2015. The re-emergence of natural products for drug discovery in the genomics era. Nat. Rev. Drug. Discov. 14, 111–129.

Huang, H., Zheng, G.S., Jiang, W.H., Hu, H.F., Lu, Y.H., 2015. One-step high-efficiency CRISPR/Cas9-mediated genome editing in *Streptomyces*. Acta Biochim. Biophys. Sin. 47, 231–243.

Iqbal, H.A., Low-Beinart, L., Obiajulu, J.U., Brady, S.F., 2016. Natural product discovery through improved functional metagenomics in *Streptomyces*. J. Am. Chem. Soc. 138, 9341–9344.

Jensen, P.R., Moore, B.S., Fenical, W., 2015. The marine actinomycete genus *Salinispora*: a model organism for secondary metabolite discovery. Nat. Prod. Rep. 32, 738–751.

Jia, B., Jin, Z.H., Lei, Y.L., Mei, L.H., Li, N.H., 2006. Improved production of pristinamycin coupled with an adsorbent resin in fermentation by *Streptomyces pristinaespiralis*. Biotechnol. Lett. 28, 1811–1815.

Jian, X.H., Pan, H.X., Ning, T.T., Shi, Y.Y., Chen, Y.S., Li, Y., Zeng, X.W., Xu, J., Tang, G.L., 2012. Analysis of YM-216391 biosynthetic gene cluster and improvement of the cyclopeptide production in a heterologous host. ACS Chem. Biol. 7, 646–651.

Jiang, W., Zhao, X., Gabrieli, T., Lou, C., Ebenstein, Y., Zhu, T.F., 2015. Cas9-Assisted Targeting of CHromosome segments CATCH enables one-step targeted cloning of large gene clusters. Nat. Commun. 6, 8101.

Jiang, Y., Chen, B., Duan, C.L., Sun, B.B., Yang, J.J., Yang, S., 2015. Multigene editing in the *Escherichia coli* genome via the CRISPR-Cas9 system. Appl. Environ. Microb. 81, 2506–2514.

Jinek, M., Chylinski, K., Fonfara, I., Hauer, M., Doudna, J.A., Charpentier, E., 2012. A programmable dual-RNA-guided DNA endonuclease in adaptive bacterial immunity. Science 337, 816–821.

Kang, H.S., Charlop-Powers, Z., Brady, S.F., 2016. Multiplexed CRISPR/Cas9 and TAR-mediated promoter engineering of natural product biosynthetic gene clusters in yeast. ACS Synth. Biol. 5, 1002–1010.

Katz, M., Hover, B.M., Brady, S.F., 2016. Culture-independent discovery of natural products from soil metagenomes. J. Ind. Microbiol. Biotechnol. 43, 129–141.

Kieser, T., Bibb, M.J., Butter, M.J., Chater, K.F., Hopwood, D.A., 2000. Practical *Streptomyces* Genetics. The John Innes Foundation, Norwich, United Kingdom.

Kim, E., Moore, B.S., Yoon, Y.J., 2015. Reinvigorating natural product combinatorial biosynthesis with synthetic biology. Nat. Chem. Biol. 11, 649–659.

Komatsu, M., Uchiyama, T., Omura, S., Cane, D.E., Ikeda, H., 2010. Genome-minimized *Streptomyces* host for the heterologous expression of secondary metabolism. Proc. Natl. Acad. Sci. 107, 2646–2651.

Li, L., Zhao, Y.W., Ruan, L.J., Yang, S., Ge, M., Jiang, W.H., Lu, Y.H., 2015. A stepwise increase in pristinamycin II biosynthesis by *Streptomyces pristinaespiralis* through combinatorial metabolic engineering. Metab. Eng. 29, 12–25.

Liu, Y., Tao, W., Wen, S., Li, Z., Yang, A., Deng, Z., Sun, Y., 2015. *In vitro* CRISPR/Cas9 system for efficient targeted DNA editing. mBio 6, e01714–e01715.

Livak, K.J., Schmittgen, T.D., 2001. Analysis of relative gene expression data using real-time quantitative PCR and the 2(T)(-Delta Delta C) method. Methods 25, 402–408.

Manderscheid, N., Bilyk, B., Busche, T., Kalinowski, J., Paululat, T., Bechthold, A.,

Petzke, L., Luzhetskyy, A., 2016. An influence of the copy number of biosynthetic gene clusters on the production level of antibiotics in a heterologous host. J. Biotechnol. 232, 110–117.
Mast, Y., Wohlleben, W., 2014. Streptogramins-two are better than one!. Int. J. Med. Microbiol. 304, 44–50.
Murakami, T., Burian, J., Yanai, K., Bibb, M.J., Thompson, C.J., 2011. A system for the targeted amplification of bacterial gene clusters multiplies antibiotic yield in *Streptomyces coelicolor*. Proc. Natl. Acad. Sci. 108, 16020–16025.
O'Connor, S.E., 2015. Engineering of secondary metabolism. Annu. Rev. Genet. 49, 71–94.
Olano, C., Lombo, F., Mendez, C., Salas, J.A., 2008. Improving production of bioactive secondary metabolites in actinomycetes by metabolic engineering. Metab. Eng. 10, 281–292.
Ongley, S.E., Bian, X., Neilan, B.A., Muller, R., 2013. Recent advances in the heterologous expression of microbial natural product biosynthetic pathways. Nat. Prod. Rep. 30, 1121–1138.
Peschke, U., Schmidt, H., Zhang, H.Z., Piepersberg, W., 1995. Molecular characterization of the lincomycin-production gene-cluster of *Streptomyces lincolnensis*-78-11. Mol. Microbiol. 16, 1137–1156.
Rutledge, P.J., Challis, G.L., 2015. Discovery of microbial natural products by activation of silent biosynthetic gene clusters. Nat. Rev. Microbiol. 13, 509–523.
Shao, Z.Y., Luo, Y.Z., Zhao, H.M., 2011. Rapid characterization and engineering of natural product biosynthetic pathways via DNA assembler. Mol. Biosyst. 7, 1056–1059.
Smanski, M.J., Zhou, H., Claesen, J., Shen, B., Fischbach, M.A., Voigt, C.A., 2016. Synthetic biology to access and expand nature's chemical diversity. Nat. Rev. Microbiol 14, 135–149.
Tanaka, Y., Kasahara, K., Hirose, Y., Murakami, K., Kugimiya, R., Ochi, K., 2013. Activation and products of the cryptic secondary metabolites biosynthetic gene clusters by rifampin resistance (*rpoB*) mutations in actinomycetes. J. Bacteriol. 195, 2959–2970.
Wang, J.W., Wang, A., Li, K., Wang, B., Jin, S., Reiser, M., Lockey, R.F., 2015. CRISPR/Cas9 nuclease cleavage combined with Gibson assembly for seamless cloning. Biotechniques 58, 161–170.
Wang, R., Mast, Y., Wang, J., Zhang, W.W., Zhao, G.P., Wohlleben, W., Lu, Y.H., Jiang, W.H., 2013a. Identification of two-component system AfsQ1/Q2 regulon and its cross-regulation with GlnR in *Streptomyces coelicolor*. Mol. Microbiol. 87, 30–48.
Wang, W.S., Li, X., Wang, J., Xiang, S.H., Feng, X.Z., Yang, K.Q., 2013b. An engineered strong promoter for streptomycetes. Appl. Environ. Microb. 79, 4484–4492.
Weber, T., Blin, K., Duddela, S., Krug, D., Kim, H.U., Bruccoleri, R., Lee, S.Y., Fischbach, M.A., Müller, R., Wohlleben, W., Breitling, R., Takano, E., Medema, M.H., 2015a. antiSMASH 3.0-a comprehensive resource for the genome mining of biosynthetic gene clusters. Nucleic Acids Res. 43, W237–W243.
Weber, T., Charusanti, P., Musiol-Kroll, E.M., Jiang, X.L., Tong, Y.J., Kim, H.U., Lee, S.Y., 2015b. Metabolic engineering of antibiotic factories: new tools for antibiotic production in actinomycetes. Trends Biotechnol. 33, 15–26.
Yanai, K., Murakami, T., Bibb, M., 2006. Amplification of the entire kanamycin biosynthetic gene cluster during empirical strain improvement of *Streptomyces kanamyceticus*. Proc. Natl. Acad. Sci. 103, 9661–9666.
Zhang, M.M., Wang, Y., Ang, E.L., Zhao, H.M., 2016. Engineering microbial hosts for production of bacterial natural products. Nat. Prod. Rep. 33, 963–987.
Zhou, T.C., Kim, B.G., Zhong, J.J., 2014. Enhanced production of validamycin A in *Streptomyces hygroscopicus* 5008 by engineering validamycin biosynthetic gene cluster. Appl. Microbiol. Biotechnol. 98, 7911–7922.